ACS OMEGA

Open Access

http://pubs.acs.org/journal/acsodf

Article

Quantitative Structure−Property Relationship Modeling with the Prediction of Physicochemical Properties of Some Novel Duchenne Muscular Dystrophy Drugs

Jyothish K and Roy Santiago*

Cite This: *ACS Omega* 2025, 10, 3640−3651

Read Online

ACCESS | Metrics & More | Article Recommendations

ABSTRACT: Duchenne muscular dystrophy is a critical, progressively worsening, and ultimately deadly illness characterized by the deterioration of skeletal muscles, respiratory failure, and heart disease. The pharmaceutical industries are persistently innovating drug design processes to address the rise of infections and effectively treat emerging syndromes or genetically based disorders with the help of quantitative structure−property relationship models. These models are mathematical tools that correlate molecular structures with their physicochemical properties through structural characteristics. Different models can be generated based on the various structural features of the compounds, and topological indices are one such significant structural feature generated from the molecular graph and are key tools used in these models. This study focuses on creating quantitative structure−property relationship models using degree-based topological indices, which are highly effective in quantitative structure−property relationship analysis to explore the diverse physicochemical properties of Duchenne muscular dystrophy drugs with the prediction of properties of a recently approved drug givinostat. Furthermore, the drug discovery and development activities can be accelerated using the developed models to forecast the possible productiveness of novel Duchenne muscular dystrophy treatment drugs.

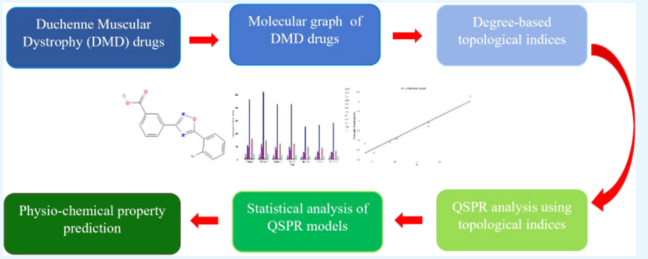

1. INTRODUCTION

Muscular dystrophy (MD) is a group of relatively rare, hereditary disorders that eventually lead to skeletal muscle atrophy and muscle weakening. There are around 30 different forms of muscular dystrophy, all of which are caused by gene mutations that impact muscle proteins that strengthen and protect muscles. The mutations usually affect specific muscle groups, resulting in different muscle damage rates, onset times, and degrees of degeneration. The numerous forms of muscular dystrophy are categorized based on the rate of general progression, the age at which symptoms first manifest, the individual skeletal muscles involved, and the inheritance pattern. The number of genes responsible for the various forms of muscular dystrophy that have been identified has significantly increased throughout the last ten years. This shift in understanding has brought about a consequential change in how muscular dystrophy is categorized, emphasizing the molecular genetic basis rather than solely relying on clinical symptoms.[1−3,10]

The identification of new skeletal muscle genes, including those involved in the extracellular matrix, sarcolemmal structure, cytoskeleton, cytosol, and nuclear membrane, has led to a re-evaluation of the phenotype-based classification system. This shift sheds light on the importance of molecular insights in understanding the pathogenesis of these disorders. The identification of dystrophin and the following studies of dystrophin−glycoprotein complex were important milestones and also acted as a first step toward understanding the molecular basis of muscular dystrophy. The dystrophin−glycoprotein complex here comprises several subunits of a linkage between the cell membrane and terminal part within the sarcolemma of skeletal muscle. Changes in dystrophin or sarcoglycans unmask this connection, causing weak membranes of the sarcolemma, making the muscle fiber prone to necrosis, which is the main pathophysiology of muscular dystrophies. Muscular dystrophy does not have a complete cure, and individuals diagnosed with the condition have to be put on a treatment plan that helps to control its progression as well as its symptoms. The chronological period in which a patient is diagnosed with muscular dystrophy depends on the onset of signs and symptoms. The following steps will be involved in the diagnosis process: the patient assessment includes taking history, symptoms, physical, and laboratory

Received: September 18, 2024
Revised: November 25, 2024
Accepted: December 18, 2024
Published: January 22, 2025

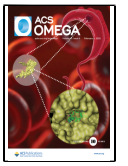

investigation like nervous conduction tests, genetic tests, and muscle biopsy.[4−8]

Muscular dystrophy has several types, although the most common one is Duchenne muscular dystrophy or Meryons disease. It is prevalent in boys, has an X-linked recessive inheritance pattern, and is caused by mutations of the dystrophin gene, which results in no expression of dystrophin protein. This disease is among the most frequent recessive diseases in the population of the human race because the frequency of this case in the global community is one in every 5000 boys. Dystrophin is a product of a gene termed DMD and is present on the gene map at locus Xp21 that is present on the X chromosome. New studies identified that the DMD gene spans 2.3 megabases, which is nearly 1% of the human genome, and according to recent discoveries, this gene is the largest in the human body. In addition, because of the size of the dystrophin gene, there is a high mutation rate in this gene, out of which 60% of mutations are deletions, and 11% involve duplications. Dystrophin is a protein containing the following domains: an N-terminal actin-binding domain, the 24 spectrin-like repeats with four hinges between the repeats, a cysteine-rich domain, and a C-terminal domain. This domain of cysteine interacts with laminin-2 through alpha and beta dystroglycan; hence, this domain essentially links the intracellular actin cytoskeleton to the extracellular matrix.[9−13]

Women typically serve as carriers of the DMD gene, while affected males seem normal at birth. However, gradual muscle deterioration and wasting begin in the proximal limb muscles before spreading to more distal muscles, leading to a diagnosis usually within the first few years of life. Early symptoms, including a waddling gait, frequent falls, difficulty moving from a sitting position (Gower's sign), and trouble climbing slopes, typically manifest between ages 2 and 3. Affected kids show reduced gross motor development and, by ages 10−12, most require a wheelchair. As muscle weakness advances, scoliosis and joint contractures develop, contributing to restrictive lung disease and necessitating assisted ventilation by about 15−20 years of age. The average intelligence of diseased boys is generally one standard deviation below the normal mean IQ, with 34.8% having intellectual disabilities. Most DMD patients die due to cardiac or respiratory failure between 20 and 30 years of age. The distribution of muscle weakness in different body parts is shown in Figure 1. Despite significant advancements in treatment over the last three decades, a full recovery from DMD is still unattainable. However, addressing DMD symptoms through a multidisciplinary approach combining medicinal, surgical, and rehabilitative treatments can considerably slow the disease's course and enhance the patient's quality of life and longevity.[14−17,21]

In the case of DMD, a timely diagnosis and early findings are critical. In laboratory examination, creatinine kinase level needs to be quantified; muscle biopsy or genetic tests are also included, and ECG would screen for cardiomyopathy. The disease can be treated with medications for controlling symptoms, muscle-strengthening exercises, special breathing techniques if someone has to experience breathing troubles, and even occupational therapy to support swallowing problems, and finally, behavioral therapy if required for the support related to the cognition part of the brain, and finally, there are gene treatments also.[11,18−21] Medications used for the treatment of DMD are prednisone, deflazacort, ataluren, casimersen, rimeporide, agamree, idebenone, and givinostat (Figure 2).

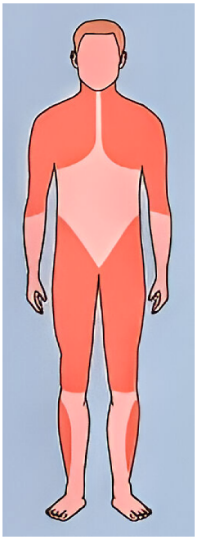

Figure 1. Duchenne muscular dystrophy affecting body parts, shown in dark colored regions (adapted with permission from Emery, A.E.H. The muscular dystrophies. *Bmj.* 317 (7164), 991−995 (1998). Copyright 1998 BMJ publishing group).

Chemical graph theory is a recognized branch of graph theory applied to describe and investigate chemical systems. In this method, molecules are represented by graphs, with atoms being the vertices and chemical bonds being the edges. With the help of such graphical representation, mathematical concepts to solve problems related to molecular structure, properties, and behavior can be applied.[22] Topological indices or molecular descriptors in chemical graph theory are quantitative measures that represent the topology or structural features of a molecular graph. These molecular descriptors contain information on the molecule's connectivity and topology and are imperative to structure−activity relation mapping, meaning predictions can be made without further testing. Some of their uses are in estimating boiling points, stability, solubility, and activity of compounds. Different types of topological indices exist according to the structural features they quantify: likely, degree-based, neighborhood-degree-based, and distance-based indices; each of these different types of indices was developed in accordance with their applications in various structural features and physicochemical properties of the molecules. Also, there are some other kinds of descriptors that were established based on different applications in quantitative structure−activity relationship (QSAR) studies, including amino acid indices based on quantum topological molecular similarity descriptors for use in the QSAR study of peptides. In drug discovery, the topological indices are used in both the QSAR and quantitative structure−property relationship (QSPR) models to identify potential drug compounds and to enhance the leading compounds. By offering quantitative descriptors of molecular properties, they greatly enhance cheminformatics, molecular modeling and design, and the discovery of novel chemical entities and potential pharmaceuticals. Additionally, they enable comprehension of molecular similarity, help in designing new chemical entities, and optimize already existing drugs, which makes them essential in the contemporary chemical and pharmaceutical sciences.[23−32]

QSAR (quantitative structure−activity relationship) and QSPR (quantitative structure−property relationship) studies

https://doi.org/10.1021/acsomega.4c08572
ACS Omega 2025, 10, 3640−3651

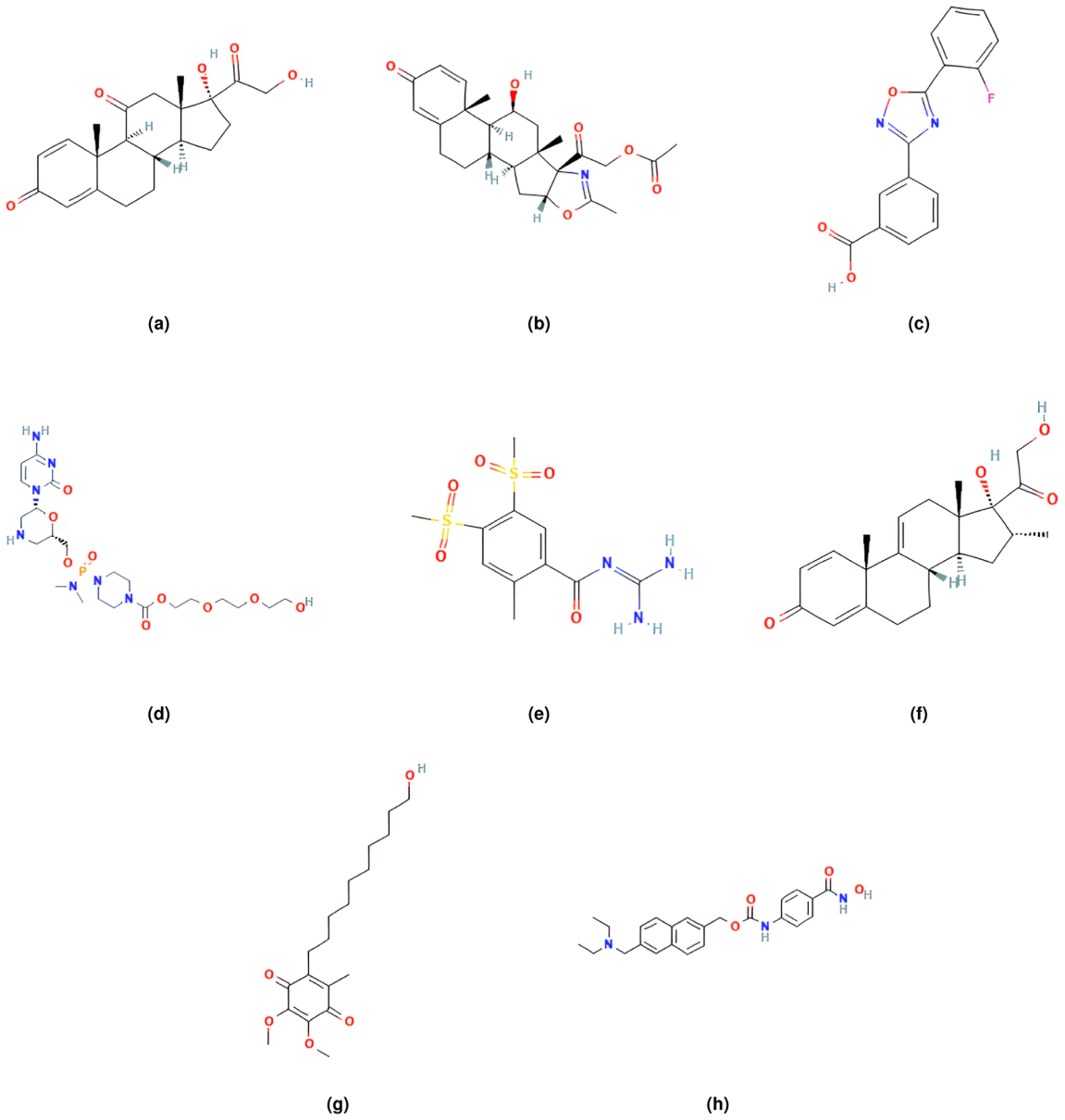

Figure 2. Molecular graph of DMD drugs: (a) prednisone; (b) deflazacort; (c) ataluren; (d) casimersen; (e) rimeporide; (f) agamree; (g) idebenone; and (h) givinostat.

are two of the most extended subfields of chemometrics or cheminformatics. QSAR and QSPR involve the use of quantitative measures to explain relationships between structures, activities, or properties of chemical systems. Variable selection, model creation, and validation evaluation are the principal steps of QSAR/QSPR analysis, and numerous improved and/or alternative approaches have been created over the past few years. These QSAR/QSPR models are indispensable in the drug discovery process since they are expected to establish the quantitative relationship between chemical structures and their respective biological activities or physical properties. There are a number of models that are comparatively equally effective to the experimental approaches, allowing them for the efficient reduction of errors in discovery phases. Using topological descriptors from chemical graph theory, these models estimate the properties of new compounds to determine the likely drug candidates. QSAR is concerned with the molecular descriptors and their relationship with biological activity to guide the design of the molecules with properties of interest while reducing undesired side effects. On the other hand, QSPR analysis estimates properties such as solubility, stability, and permeability, which are crucial for formulating a drug, getting it into the body, and its general advancement. Hence, QSAR and QSPR analyses substantially decrease the actual experiments required, shorten the time taken during drug discovery, and increase the efficacy of identifying the new drugs that are safe to use and effective in the treatment of diseases. This not only saves time and resources but also is useful in alerting for possible drug candidates of good properties during the early stages of the forming phase of the new drug development process so that the lead compounds in preparation of novel drugs can be optimized more effectively. Their ability to predict the issues on toxicity, efficiency, and pharmacodynamics makes QSAR/QSPR models irreplaceable in the designing of the new drugs.[33−40]

https://doi.org/10.1021/acsomega.4c08572
ACS Omega 2025, 10, 3640−3651

Over the years, various drugs have been introduced to treat DMD due to the increasing number of affected individuals and the disease's rapid progression. While some drugs have shown positive results in trials, others have failed to pass all clinical trials and obtain approval. This study is significant as it examines the physicochemical properties of certain drugs used for DMD treatment and correlates these properties with topological indices to develop QSAR/QSPR models. Using these models, we evaluated the physicochemical properties of the recently FDA-approved drug givinostat and assessed its effectiveness in treating DMD through topological analysis of the molecular graph of the drugs used for DMD treatment.

2. PRELIMINARIES

A molecular graph represents a molecule by depicting atoms as vertices (nodes) and chemical bonds as edges (lines). Molecular graphs provide a simplified yet informative framework for studying the structure, properties, and behavior of molecules using mathematical and computational methods. In this study, we have considered only simple, connected graphs represented by $G = [V(G), E(G)]$, where $V(G)$ is the vertex set and $E(G)$ is the edge set of the graph G. The degree of a vertex v is denoted by d_v, which is the total number of edges adjacent to the vertex $v \in V(G)$.[22,41]

2.1. Topological Indices. In 1947, Harold Wiener's investigation on the steaming limit of paraffin gave rise to the idea of the topological index. Numerous topological indices have been developed over the years due to their wide range of applications in drug development, material and polymer research, QSAR/QSPR analysis, and other fields. There are several forms of these indices, and each focuses on some aspect of the molecular structure. Some analyze how many connections there are between each atom, such as degree-based indices. Others rely on the shortest paths between atoms, such as distance-based indices.[23,24] In this study, we have employed 12 degree-based topological descriptors to develop a predictive model for the physicochemical characteristics of drugs used to treat Duchenne muscular dystrophy.

Gutman and Trinajstić investigated the effect of total π-electron energy on the molecular structure using a numerical approach. The Zagreb index, one of the earliest graph invariants, was initially introduced in 1972 and further developed in 1975.[42,43] For a graph G, the first and second Zagreb indices (M_1 and M_2) are defined as follows

$$M_1(G) = \sum_{uv \in E(G)} [d_u + d_v]$$

$$M_2(G) = \sum_{uv \in E(G)} [d_u \times d_v]$$

The Randić index (R index) was proposed in 1975 by the scientist Milan Randić.[44] The Randić index is frequently referred to as the "connectivity index". It is the most widely used and useful formula, demonstrating a strong correlation with most molecular graph features. It is computed as follows

$$R(G) = \sum_{uv \in E(G)} \left[\frac{1}{\sqrt{d_u d_v}}\right]$$

The reciprocal Randić index (RR index) was introduced by Gutman et al. in 2014. This variant of the original Randić index was designed to offer an alternative method for evaluating molecular branching and connectivity within chemical graph theory.[45] The mathematical expression for the calculation of the reciprocal Randić index is

$$\mathrm{RR}(G) = \sum_{uv \in E(G)} [\sqrt{d_u d_v}]$$

The augmented Zagreb index (AZ index) was developed in 2014 by Ali et al.[46] and is given by

$$\mathrm{AZ}(G) = \sum_{uv \in E(G)} \left[\frac{d_u \times d_v}{d_u + d_v - 2}\right]$$

A modified version of the Zagreb index called the hyper Zagreb index (HM index) was introduced by Shirdel et al. in 2013,[47] which is defined as

$$\mathrm{HM}(G) = \sum_{uv \in E(G)} [d_u + d_v]^2$$

In the 1980s, Siemion Fajtlowicz developed a computer program designed to automatically generate hypotheses in graph theory. Through this program, he explored potential connections among numerous graph invariants, including a vertex-degree-based variable. Later, in 2012, Zhang identified this previously unknown variable and named it the harmonic index (H index).[48,49] The formula of the harmonic index is defined as

$$H(G) = \sum_{uv \in E(G)} \left[\frac{2}{d_u + d_v}\right]$$

In 2009, Vukicevic and Furtula introduced the geometric–arithmetic index (GA index), an advanced version of the Randić index.[50] They found that for some physicochemical factors, such as enthalpy of vaporization, entropy, and the acentric factor, the GA index is more effective than the Randić index. The GA index is defined as

$$\mathrm{GA}(G) = \sum_{uv \in E(G)} \left[\frac{2\sqrt{d_u d_v}}{d_u + d_v}\right]$$

In 2009, Zhou and Trinajstic introduced the sum connectivity index (SC-index), and then it was subsequently evaluated and implemented in 2011,[51] which is defined as

$$\mathrm{SC}(G) = \sum_{uv \in E(G)} \left[\frac{1}{\sqrt{d_u + d_v}}\right]$$

In 2010, Vukievi and Gaperov introduced the symmetric division index (AZI index) as part of an effort to enhance numerous QSPR/QSAR investigations. They explored a new category of molecular descriptors known as discrete Adriatic indices, comprising 148 descriptors, but found that only a small subset of these descriptors proved useful. Among these, the AZI index emerged as a valuable discrete Adriatic index. Currently, it is recognized as having the strongest correlation capability among all molecular descriptors for calculating the total surface area of polychlorobiphenyls.[52,53] The AZI index is determined as

$$\mathrm{AZI}(G) = \sum_{uv \in E(G)} \left[\frac{d_u^2 + d_v^2}{d_u d_v}\right]$$

https://doi.org/10.1021/acsomega.4c08572
ACS Omega 2025, 10, 3640−3651

Table 1. Physicochemical Properties of DMD Drugs

drugs	molecular formula	molecular weight (g/mol)	enthalpy of vaporization (kJ/mol)	molar refractivity (cm^3)	polarizability (cm^3)	molar volume (cm^3)	melting point (°C)
prednisone	$C_{21}H_{26}O_5$	358.428	98.7 ± 6.0	94.1 ± 0.4	37.3 ± 0.5 × 10^{-24}	273.6 ± 5.0	213.56
deflazacort	$C_{25}H_{31}NO_6$	441.517	101.8 ± 6.0	115.1 ± 0.5	45.6 ± 0.5 × 10^{-24}	311.6 ± 7.0	229.78
ataluren	$C_{15}H_9FN_2O_3$	284.242	81.4 ± 3.0	70.8 ± 0.3	28.1 ± 0.5 × 10^{-24}	206.0 ± 3.0	190.86
casimersen	$C_{22}H_{40}N_7O_9P$	577.568	121.6 ± 6.0	137.0 ± 0.5	54.3 ± 0.5 × 10^{-24}	390.2 ± 7.0	
rimeporide	$C_{11}H_{15}N_3O_5S_2$	333.384	103.3 ± 3.0	77.4 ± 0.5	30.7 ± 0.5 × 10^{-24}	214.8 ± 7.0	224.68
agamree	$C_{22}H_{28}O_4$	356.455	95.2 ± 6.0	98.3 ± 0.4	39.0 ± 0.5 × 10^{-24}	286.1 ± 5.0	203.94
idebenone	$C_{19}H_{30}O_5$	338.439	88.1 ± 6.0	92.1 ± 0.4	36.5 ± 0.5 × 10^{-24}	312.1 ± 5.0	192.68
givinostat	$C_{24}H_{27}N_3O_4$	421.489		122.3 ± 0.3	48.5 ± 0.5 × 10^{-24}	334.6 ± 3.0	278.81

In 2010, Vukicevic introduced the inverse sum index (IS index). In 2015, the IS index was analyzed to identify its extreme values across different graph categories, such as linked graphs, molecular graphs, trees, and chemical trees,[54] which is defined as

$$\mathrm{IS}(G) = \sum_{uv \in E(G)} \left[\frac{d_u d_v}{d_u + d_v} \right]$$

In 1998, Estrada and Torres introduced a new degree-based topological index named the atom-bond connectivity index. This index, often abbreviated as the ABC index, shows a strong correlation with the thermochemical properties of alkanes, especially with their heat of formation.[55] The ABC index is determined as

$$\mathrm{ABC}(G) = \sum_{uv \in E(G)} \left[\sqrt{\frac{d_u + d_v - 2}{d_u d_v}} \right]$$

2.2. Duchenne Muscular Dystrophy Drugs. Glucocorticosteroids, including deflazacort and prednisone, are among the most commonly used drugs for the treatment of DMD patients. These can help in increasing total muscle mass and strength in DMD patients by stimulating insulin-like growth factors, reducing inflammation, decreasing lymphocyte activity, promoting myoblast proliferation, and cytokine production.[56,57]

Prednisone is a synthetic glucocorticosteroid that is used for its effective anti-inflammatory and immunomodulating properties. However, it will bind with the cell surface receptors and then be transported to the nucleus once it gets to the cell, where it is docked and then triggers certain nuclear receptors. This interaction results in the altering of gene expression and the suppression of the synthesis of proinflammatory cytokines.[56,58]

Deflazacort or Emflaza is one type of glucocorticoid categorized under acetonide or an *O*-isopropylidene derivative. It has anti-inflammatory activity and was originally patented in 1969 and then given authorization for medical use, which was allowed in the year 1985. The U.S. Food and Drug Administration (FDA) approved deflazacort in 2017 for use in the treatment of DMD, and it can be considered a first-class treatment for Duchenne muscular dystrophy.[57,59]

Ataluren is used to treat DMD in ambulatory patients aged five and older. This oral small molecule targets nonsense mutations by promoting ribosomal read-through, allowing the translation process to bypass the mutation and produce a functional dystrophin protein. The European Medicines Agency has approved ataluren for use in patients with DMD caused by specific genetic defects in the dystrophin gene.[60]

Casimersen is an antisense oligonucleotide used to treat DMD in patients with a confirmed dystrophin gene mutation that allows for exon-45 skipping. Proposed for use as a medicine in the United States in 2021, casimersen is the first FDA-approved targeted treatment for individuals with a mutation in the DMD gene amenable to exon skipping.[61]

Rimeporide, a derivative of benzoyl guanidine, serves as a strong and specific inhibitor of sodium proton exchanger isoform-1 (NHE-1), which is found in all of the body's cell membranes. NHE-1 inhibitor rimeporide, which was first developed for cardiac therapeutic purposes, is now going through testing to see if it could potentially be used to treat cardiomyopathy in DMD patients. It was approved by the FDA in 2017.[62]

Agamree is an innovative corticosteroid designed to enhance motor function in DMD patients. It operates by reducing inflammation through inhibition of cytokine production, which is a protein that trigger inflammation. In addition to its motor function benefits, agamree may offer advantages such as reduced impact on bone health, growth rate, and behavior compared to those of traditional corticosteroids. Vamorolone, the active compound in agamree, exerts its anti-inflammatory and immunosuppressive effects by acting on the glucocorticoid receptor. Agamree received FDA approval in 2023, marking a significant milestone in DMD treatment.[63,64]

Idebenone is a possible medication for DMD that aims to slow down the deterioration in respiratory function. In DMD, respiratory muscle weakening is a primary cause of premature mortality and carries significant dangers, frequently resulting in life-threatening consequences. Studies have shown that idebenone significantly attenuates the decline in respiratory function among DMD patients aged 8−18 years who are not concurrently using glucocorticoids. These findings suggest that idebenone has the potential to alter the natural progression of respiratory disease in DMD, addressing a critical need in clinical management where respiratory decline remains a primary cause of morbidity and mortality.[65,66]

Givinostat (Duvyzat) is an oral medication approved by the FDA in March 2024 for treating DMD in patients aged six and older. It is the first nonsteroidal drug approved for all genetic variants of DMD. As a histone deacetylase (HDAC) inhibitor, givinostat targets pathogenic processes to reduce inflammation and muscle loss. HDACs are enzymes that regulate gene activity within cells and can obstruct muscle regeneration in DMD. By acting on the downstream effects of genetic defects, givinostat has the potential to treat the entire DMD patients.[67,68]

Prednisone, deflazacort, ataluren, casimersen, rimeporide, agamree, idebenone, and givinostat (Figure 2) are the pre-existing medications for the treatment of DMD that are taken

https://doi.org/10.1021/acsomega.4c08572
ACS Omega 2025, 10, 3640−3651

Table 2. Edge Partition of DMD Drugs

drugs	$E_{(1,2)}$	$E_{(1,3)}$	$E_{(1,4)}$	$E_{(2,2)}$	$E_{(2,3)}$	$E_{(2,4)}$	$E_{(3,3)}$	$E_{(3,4)}$	$E_{(4,4)}$
prednisone	1	3	3	3	8	3	3	4	1
deflazacort		6	2	3	13	3	3	5	1
ataluren		3		6	10		4		
casimersen	1	5	1	14	14	1	3	2	
rimeporide		4	6		6		3	2	
agamree	1	3	3	3	9	2	2	5	1
idebenone	3	3		9	3		6		
givinostat	3	2		5	21		2		

into consideration for the development of the predictive models. These medications experimental physicochemical characteristics, including their molecular weight, molar refractivity, enthalpy of vaporization, polarizability, molar volume, and melting point, are listed in Table 1. The sources of these data are obtained from ChemSpider and PubChem.[72,73]

2.3. Regression Analysis. Regression analysis is a statistical method that can be used to get the relations between some variables and that forms an equation based on the observed values. It is used to explain the nature of the association that exists between the dependent variable and one or more independent variables, where the focus is on the extent of change in the dependent variable concerning the change in the independent variable.[69] Simple regression has one dependent and one independent variable, while in multiple regression, there is the possibility to have several independent variables. From here, it is intended for a predictive model, whereby the values of independent variables are already known, as well as for explanatory objectives that reveal the relationships between variables. Regression analysis is used widely in different academic disciplines including economics, medicine, social studies, and engineering for purposes of analysis, prediction, and decision-making. It depends on assumptions such as data linearity, independent observations, consistent error variance, and normal error distribution, ensuring robust and dependable outcomes under these conditions.[70,71]

3. METHODOLOGY

We have used analytical approaches, graph theoretical methods, degree counting methods, and edge partition methodology for the calculation of the topological indices. Using the statistical program SPSS, the correlation coefficients between topological indices and DMD drug properties were determined, and predictive models were created with the aid of regression analysis. MATLAB software has been utilized for computation of mathematical equations and verification as well. Microsoft Power BI has been used to create the 2D graphs showing comparisons between topological indices and compounds properties.

4. RESULTS AND DISCUSSION

In this section, we have computed the 12 degree-based topological descriptors, including the first and second Zagreb indices, Randić index, reciprocal Randić index, geometric−arithmetic index, augmented Zagreb index, hyper Zagreb index, harmonic index, sum connectivity index, symmetric division index, inverse sum index, and atom-bond connectivity index of Duchenne muscular dystrophy drugs from their corresponding molecular graphs, which are simple connected graphs with a degree maximum of 4 and minimum of 1. The corresponding edge partition of the molecular graph of these Duchenne muscular dystrophy drugs is given below in Table 2.

Theorem 4.1: Let G be the molecular graph of the prednisone drug. Then,

i $M_1(G) = 154$
ii $M_2(G) = 198$
iii $R(G) = 12.1705$
iv $\mathrm{RR}(G) = 73.548$
v $\mathrm{AZ}(G) = 245.6669$
vi $\mathrm{HM}(G) = 856$
vii $H(G) = 11.4595$
viii $\mathrm{GA}(G) = 27.5667$
ix $\mathrm{SC}(G) = 12.8116$
x $\mathrm{AZI}(G) = 72.4167$
xi $\mathrm{IS}(G) = 35.2738$
xii $\mathrm{ABC}(G) = 20.8485$

Proof: The total edge set cardinality of the molecular graph G of the prednisone drug is 29, and its partition is given in Table 2. So, by using this partition and the topological index equations in the previous section, we obtain that

$$M_1(G) = 1 \times (1+2) + 3 \times (1+3) + 3 \times (1+4) + 3 \times (2+2) + 8 \times (2+3) + 3 \times (2+4) + 3 \times (3+3) + 4 \times (3+4) + 1 \times (4+4) = 154$$

$$M_2(G) = 1 \times (1 \times 2) + 3 \times (1 \times 3) + 3 \times (1 \times 4) + 3 \times (2 \times 2) + 8 \times (2 \times 3) + 3 \times (2 \times 4) + 3 \times (3 \times 3) + 4 \times (3 \times 4) + 1 \times (4 \times 4) = 198$$

$$R(G) = 1 \times \left(\frac{1}{\sqrt{1 \times 2}}\right) + 3 \times \left(\frac{1}{\sqrt{1 \times 3}}\right) + 3 \times \left(\frac{1}{\sqrt{1 \times 4}}\right) + 3 \times \left(\frac{1}{\sqrt{2 \times 2}}\right) + 8 \times \left(\frac{1}{\sqrt{2 \times 3}}\right) + 3 \times \left(\frac{1}{\sqrt{2 \times 4}}\right) + 3 \times \left(\frac{1}{\sqrt{3 \times 3}}\right) + 4 \times \left(\frac{1}{\sqrt{3 \times 4}}\right) + 1 \times \left(\frac{1}{\sqrt{4 \times 4}}\right) = 12.1705$$

$$\mathrm{RR}(G) = 1 \times \sqrt{1 \times 2} + 3 \times \sqrt{1 \times 3} + 3 \times \sqrt{1 \times 4} + 3 \times \sqrt{2 \times 2} + 8 \times \sqrt{2 \times 3} + 3 \times \sqrt{2 \times 4} + 3 \times \sqrt{3 \times 3} + 4 \times \sqrt{3 \times 4} + 1 \times \sqrt{4 \times 4} = 73.548$$

https://doi.org/10.1021/acsomega.4c08572
ACS Omega 2025, 10, 3640−3651

Table 3. Topological Indices Values of DMD Drugs

drugs	M_1	M_2	R	RR	AZ	HM	H	GA	SC	AZI	IS	ABC
prednisone	154	198	12.1705	73.548	245.6669	856	11.4595	27.5667	12.8116	72.4167	35.2738	20.8485
deflazacort	190	243	15.0254	91.0415	299.2456	1044	14.1786	34.3106	15.9011	88.5833	43.7714	25.9059
ataluren	110	129	10.1479	53.691	183.6875	538	9.8333	22.396	10.6051	51.6667	26.25	16.4299
casimersen	192	220	18.7402	93.124	321.0652	930	18.0714	39.7124	19.1745	94.4167	45.2786	29.4527
rimeporide	108	123	9.3362	49.5533	137.5421	570	8.3714	19.1224	9.3472	62	22.9286	15.9958
agamree	154	199	12.1805	73.6331	248.1003	858	11.4786	27.5934	12.8203	72.1667	35.3548	20.8274
idebenone	108	123	11.5781	52.7873	198.4688	510	11.2	23.3659	11.5232	54	25.85	17.0561
givinostat	154	176	15.0159	75.146	261.5312	736	14.5667	32.1362	15.44	73.6667	36.7	23.4724

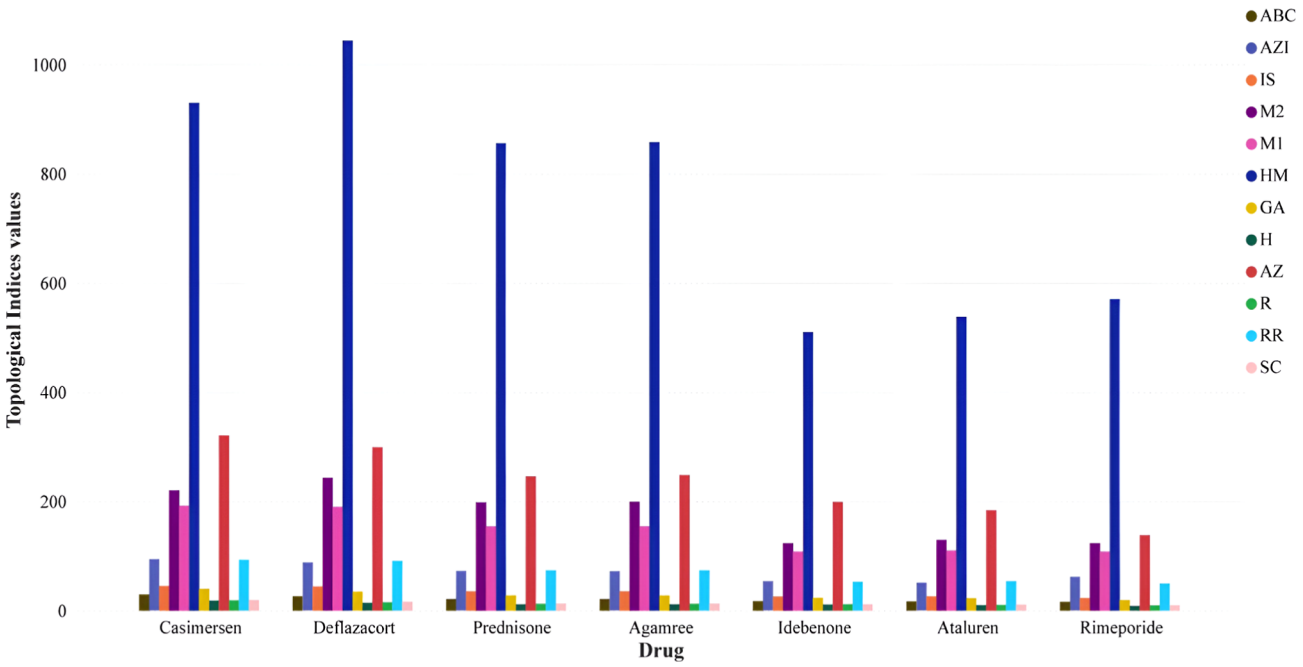

Figure 3. 3D representation of topological indices of DMD drugs.

$$\mathrm{AZ}(G) = 1 \times \left(\frac{1 \times 2}{1 + 2 - 2}\right)^3 + 3 \times \left(\frac{1 \times 3}{1 + 3 - 2}\right)^3 + 3 \times \left(\frac{1 \times 4}{1 + 4 - 2}\right)^3 + 3 \times \left(\frac{2 \times 2}{2 + 2 - 2}\right)^3 + 8 \times \left(\frac{2 \times 3}{2 + 3 - 2}\right)^3 + 3 \times \left(\frac{2 \times 4}{2 + 4 - 2}\right)^3 + 3 \times \left(\frac{3 \times 3}{3 + 3 - 2}\right)^3 + 4 \times \left(\frac{3 \times 4}{3 + 4 - 2}\right)^3 + 1 \times \left(\frac{4 \times 4}{4 + 4 - 2}\right)^3 = 245.6669$$

$$\mathrm{HM}(G) = 1 \times (1 + 2)^2 + 3 \times (1 + 3)^2 + 3 \times (1 + 4)^2 + 3 \times (2 + 2)^2 + 8 \times (2 + 3)^2 + 3 \times (2 + 4)^2 + 3 \times (3 + 3)^2 + 4 \times (3 + 4)^2 + 1 \times (4 + 4)^2 = 856$$

$$H(G) = 1 \times \left(\frac{2}{1 + 2}\right) + 3 \times \left(\frac{2}{1 + 3}\right) + 3 \times \left(\frac{2}{1 + 4}\right) + 3 \times \left(\frac{2}{2 + 2}\right) + 8 \times \left(\frac{2}{2 + 3}\right) + 3 \times \left(\frac{2}{2 + 4}\right) + 3 \times \left(\frac{2}{3 + 3}\right) + 4 \times \left(\frac{2}{3 + 4}\right) + 1 \times \left(\frac{2}{4 + 4}\right) = 11.4595$$

$$\mathrm{GA}(G) = 1 \times \left(\frac{2\sqrt{1 \times 2}}{1 + 2}\right) + 3 \times \left(\frac{2\sqrt{1 \times 3}}{1 + 3}\right) + 3 \times \left(\frac{2\sqrt{1 \times 4}}{1 + 4}\right) + 3 \times \left(\frac{2\sqrt{2 \times 2}}{2 + 2}\right) + 8 \times \left(\frac{2\sqrt{2 \times 3}}{2 + 3}\right) + 3 \times \left(\frac{2\sqrt{2 \times 4}}{2 + 4}\right) + 3 \times \left(\frac{2\sqrt{3 \times 3}}{3 + 3}\right) + 4 \times \left(\frac{2\sqrt{3 \times 4}}{3 + 4}\right) + 1 \times \left(\frac{2\sqrt{4 \times 4}}{4 + 4}\right) = 27.5667$$

$$\mathrm{SC}(G) = 1 \times \left(\frac{1}{\sqrt{1 + 2}}\right) + 3 \times \left(\frac{1}{\sqrt{1 + 3}}\right) + 3 \times \left(\frac{1}{\sqrt{1 + 4}}\right) + 3 \times \left(\frac{1}{\sqrt{2 + 2}}\right) + 8 \times \left(\frac{1}{\sqrt{2 + 3}}\right) + 3 \times \left(\frac{1}{\sqrt{2 + 4}}\right) + 3 \times \left(\frac{1}{\sqrt{3 + 3}}\right) + 4 \times \left(\frac{1}{\sqrt{3 + 4}}\right) + 1 \times \left(\frac{1}{\sqrt{4 + 4}}\right) = 12.8116$$

$$\mathrm{AZI}(G) = 1 \times \left(\frac{1^2 + 2^2}{1 \times 2}\right) + 3 \times \left(\frac{1^2 + 3^2}{1 \times 3}\right) + 3 \times \left(\frac{1^2 + 4^2}{1 \times 4}\right) + 3 \times \left(\frac{2^2 + 2^2}{2 \times 2}\right) + 8 \times \left(\frac{2^2 + 3^2}{2 \times 3}\right) + 3 \times \left(\frac{2^2 + 4^2}{2 \times 4}\right) + 3 \times \left(\frac{3^2 + 3^2}{3 \times 3}\right) + 4 \times \left(\frac{3^2 + 4^2}{3 \times 4}\right) + 1 \times \left(\frac{4^2 + 4^2}{4 \times 4}\right) = 72.4167$$

https://doi.org/10.1021/acsomega.4c08572
ACS Omega 2025, 10, 3640−3651

Table 4. Correlation Values of Properties of DMD Drugs with Indices

	molecular weight (g/mol)	enthalpy of vaporization (kJ/mol)	molar refractivity (cm^3)	polarizability (cm^3)	molar volume (cm^3)	melting point (°C)
M_1	0.8381	0.8951	0.7033	0.8951	0.7410	0.5788
M_2	0.7120	0.8041	0.5863	0.8041	0.6502	0.5479
R	0.9667	0.9793	0.7659	0.9794	0.9207	0.3854
RR	0.8428	0.9040	0.6835	0.9041	0.7616	0.5250
AZ	0.8301	0.9186	0.5930	0.9187	0.8417	0.2891
HM	0.6966	0.7803	0.6109	0.7804	0.6100	0.6170
H	0.9512	0.9675	0.7264	0.9676	0.9250	0.2684
GA	0.9253	0.9608	0.7173	0.9609	0.8652	0.4007
SC	0.9502	0.9730	0.7438	0.9731	0.8951	0.3911
AZI	0.9048	0.9166	0.8456	0.9167	0.7469	0.7673
IS	0.8448	0.9092	0.6652	0.9093	0.7772	0.4760
ABC	0.9431	0.9640	0.7835	0.9641	0.8414	0.5607

$$\mathrm{IS}(G) = 1 \times \left(\frac{1 \times 2}{1 + 2}\right) + 3 \times \left(\frac{1 \times 3}{1 + 3}\right) + 3 \times \left(\frac{1 \times 4}{1 + 4}\right) + 3 \times \left(\frac{2 \times 2}{2 + 2}\right) + 8 \times \left(\frac{2 \times 3}{2 + 3}\right) + 3 \times \left(\frac{2 \times 4}{2 + 4}\right) + 3 \times \left(\frac{3 \times 3}{3 + 3}\right) + 4 \times \left(\frac{3 \times 4}{3 + 4}\right) + 1 \times \left(\frac{4 \times 4}{4 + 4}\right) = 35.2738$$

$$\mathrm{ABC}(G) = 1 \times \sqrt{\frac{1 + 2 - 2}{1 \times 2}} + 3 \times \sqrt{\frac{1 + 3 - 2}{1 \times 3}} + 3 \times \sqrt{\frac{1 + 4 - 2}{1 \times 4}} + 3 \times \sqrt{\frac{2 + 2 - 2}{2 \times 2}} + 8 \times \sqrt{\frac{2 + 3 - 2}{2 \times 3}} + 3 \times \sqrt{\frac{2 + 4 - 2}{2 \times 4}} + 3 \times \sqrt{\frac{3 + 3 - 2}{3 \times 3}} + 4 \times \sqrt{\frac{3 + 4 - 2}{3 \times 4}} + 1 \times \sqrt{\frac{4 + 4 - 2}{4 \times 4}} = 20.8485$$

The topological indices for each of the eight drugs used to treat DMD are determined using the same methodology as that used before, and the results are given in Table 3. The graphical visualization of these index values is shown in Figure 3. From these graphical visualizations, it is clear that the symmetric division index (AZI index) has the highest numerical values and the harmonic index (H index) has the lowest numerical values for all the drugs.

4.1. Numerical Analysis of Topological Indices. Table 4 presents the estimated correlation coefficients between the DMD medications' topological indices and physicochemical properties. To determine the correlation in this instance, we have used Microsoft Excel. The table displays the highest correlation for each property, which indicates the predictive power of each index with the physicochemical properties. That is, the highest correlation coefficient indicates the higher predictive ability of the index with that particular property. Molecular weight, enthalpy of vaporization, and polarizability have the strongest correlations with the Randić index. Likewise, molar refractivity and melting point have the highest correlation with the symmetric division index, and the harmonic index exhibits the highest correlations with molar volume. In Figure 4, the correlation between each topological index and the physicochemical properties is shown graphically.

By analyzing both Table 4 and Figure 4, we can deduce that the Randić index appears to be the most reliable method for predicting the molecular weight, enthalpy of vaporization, and polarizability since we can see that out of the 12 topological indices computed, the Randić index shows a high correlation value with these properties. The symmetric division index has good predictive power on molar refractivity and melting point. For molar volume, the harmonic index is the best predictor. Figure 5 displays scatter plots for the best prediction pairs. And from these plots, it is clear that all the computed degree-based topological descriptors show a significant positive correlation with the physicochemical characteristics of DMD drugs.

4.2. Quantitative Structure−Property Relationship (QSPR) Analysis of DMD Drugs. In this section, QSPR analysis has been performed using the topological indices and physicochemical properties of DMD drugs, including molecular weight (MW), enthalpy of vaporization (ΔH_{vap}), molar refractivity (R_m), polarizability (α), molar volume (V_m), and melting point (MP). We have used the linear regression model to generate the predictive QSPR model. Regression analysis is carried out using SPSS software on the best-predicting combinations, generating QSPR models. The linear regression model is given by

$$P = A + B(\mathrm{TI})$$

where A denotes the constant, B is the regression coefficient, TI stands for the topological index, and P denotes the physicochemical characteristics of the DMD drugs. When the value of TI = 0, the constant term A equals the value of P. Here, all topological indices are positive and nonzero. The regression line's slope, B, shows how the dependent parameter P (representing experimental chemical and physical properties) changes with each unit variation in the independent variable topological index (TI). The high correlation coefficient values between the estimated and experimental values of DMD drugs demonstrate the effectiveness of these calculations.

The QSPR models for the various physicochemical properties of DMD drugs with the best-fitting topological indices are given by

$$\text{Molecular weight} = 29.368(R) + 10.142$$

$$\text{Molar refractivity} = 6.87(\mathrm{AZI}) + 10.307$$

$$\text{Enthalpy of vaporization} = 0.661(R) + 51.849$$

$$\text{Polarizability} = 2.719(R) + 4.146$$

https://doi.org/10.1021/acsomega.4c08572
ACS Omega 2025, 10, 3640−3651

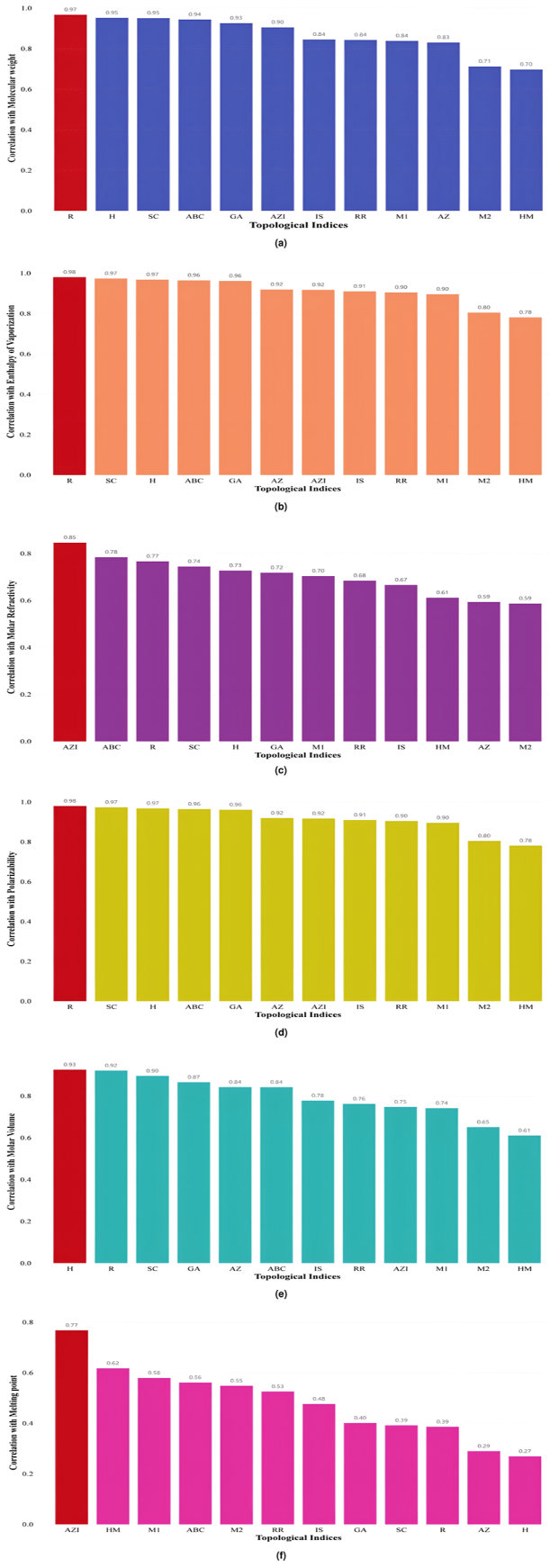

Figure 4. Bar plot of correlation values of physicochemical properties with various topological indices: (a) MW; (b) ΔH_{vap}; (c) R_m; (d) α; (e) V_m; and (f) MP.

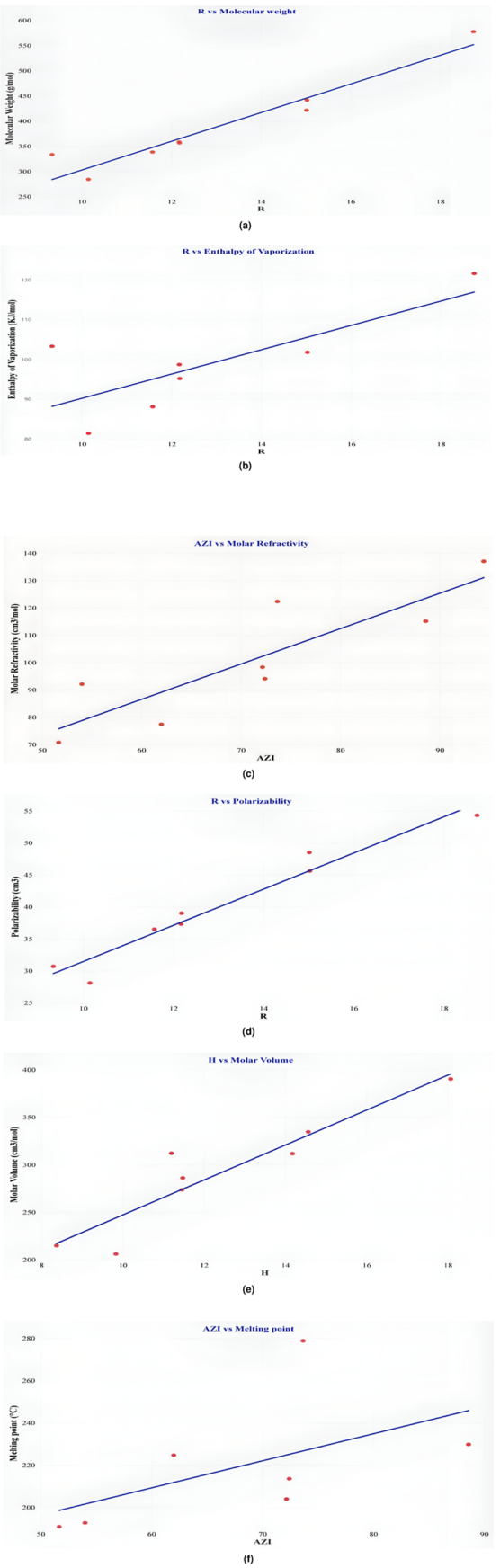

Figure 5. Scatter plots with best fit lines: (a) R vs MW; (b) R vs ΔH_{vap}; (c) AZI vs R_m; (d) R vs α; (e) H vs V_m; and (f) AZI vs MP.

https://doi.org/10.1021/acsomega.4c08572
ACS Omega 2025, 10, 3640−3651

Table 5. Statistical Parameters for the Linear QSPR Models

property	topological index	B	A	r	r^2	p	t
molecular weight	R	29.368	10.142	0.967	0.935	⟨0.001	8.446
molar refractivity	AZI	6.87	10.307	0.979	0.959	⟨0.001	10.813
enthalpy of vaporization	R	0.661	51.849	0.846	0.715	0.017	3.542
polarizability	R	2.719	4.146	0.979	0.959	⟨0.001	10.832
molar volume	H	18.252	64.34	0.921	0.848	0.003	5.287
melting point	AZI	0.904	148.874	0.767	0.589	0.075	2.393

$$\text{Molar volume} = 18.252(H) + 64.34$$

$$\text{Melting point} = 0.904(\text{AZI}) + 148.874$$

4.3. Statistical Analysis of QSPR Models. Different parameters in a regression model perform various purposes (refer to Table 5). The significance of the obtained data is indicated by the value of p. The p-value is a crucial statistic in regression analysis that helps to assess the importance of each individual predictor in the model. It shows the likelihood that the observed correlation between the dependent variable and the predictor occurred by chance or not. A statistically significant influence of the related predictor on the dependent variable is indicated by a low p-value, usually less than 0.05. This indicates that there is substantial evidence that the predictor makes a significant contribution to the model. A high p-value, on the other hand, suggests that the predictor is not statistically significant and might not make a significant contribution to the explanation of the variance in the dependent variable. The constant is represented by the number A, and the coefficient is represented by the number B. The correlation coefficient between the calculated and experimental values of the physical attributes is represented by the number r. It is possible for the values of r to be negative (inverse relation) or positive (direct relation). r^2 provides an assessment of the relationship between an independent variable's changes and a dependent variable's. It does not say anything about how accurate the data and estimations are or how accurate the chosen model is. The t-value is an essential statistic in regression analysis; it is used to evaluate each regression coefficient's significance individually. It provides information about the strength and direction of the link between the predictor and the dependent variable by calculating the number of standard errors the coefficient deviates from zero. A high absolute t-value implies a significant difference between the predictor and zero, implying considerable influence on the dependent variable. Any absolute t-value greater than 2 is generally considered acceptable. Our level of confidence in the coefficient as a predictor increases with the t-value. By analyzing t-values, researchers may determine which variables add a lot to the model and decide which predictors to include or leave out, which improves the accuracy and interpretability of the model.[37,69−71]

So, by analyzing Table 5, all the prediction models have the accepted range of t-values, but the melting point prediction model has a significance value; the p-value is greater than 0.05. Hence, we omit the melting point regression model from analysis; the rest of the model shows the significance value within the range. So, the QSPR prediction models of molecular weight, enthalpy of vaporization, molar refractivity, polarizability, and molar volume have been considered.

4.4. Physicochemical Characteristics Prediction and Analysis of the Givinostat Drug. Givinostat is a newly discovered and approved drug by the FDA in 2024 for treating DMD disease (refer to Figure 2h). The physicochemical properties and topological index values of the drug givinostat are given in Tables 1 and 3, respectively. In this section, we have tried to predict the physicochemical properties of the givinostat drug using the generated QSPR prediction models. The QSPR analysis has vast applications in the pharmaceutical and drug industry. One of the major issues of developing a new drug is identifying the right main compound with desired properties; otherwise, the developed drug may fail to accomplish its purpose. Hence, these QSPR models often help scientists to choose the right compound for developing the new drug with desired properties or to realize the range of values of the specific properties.

Hence, by using these QSPR prediction models, we have computed the physicochemical properties of the drug givinostat; refer to Table 6, which shows both the predicted and experimental values of physicochemical properties. By analyzing Table 6, it is clear that our predicted values and experimental values are approximate within a closed range, which shows the higher predictive ability of the generated QSPR models. So, by using these models, scientists who are working in drug discovery can scrutinize the prime compounds for developing new drugs with desired properties.

Table 6. Givinostat Properties Comparison

property	experimental value	predicted value
molecular weight (g/mol)	421.489	451.132
molar refractivity (cm^3)	122.3 ± 0.3	113.466
enthalpy of vaporization (kJ/mol)		100.543
polarizability (cm^3)	$48.5 \pm 0.5 \times 10^{-24}$	44.974×10^{-24}
molar volume (cm^3)	334.6 ± 3.0	330.217

5. CONCLUSIONS

In the field of pharmaceutical drug design, the identification of molecular structural characteristics is crucial for the successful development of novel products. Such features can be obtained using quantitative structure−property relationship modeling with topological indices. Several promising drugs used for the treatment of Duchenne muscular dystrophy, such as prednisone, deflazacort, ataluren, casimersen, rimeporide, agamree, and idebenone, are studied along with the newly approved drug givinostat, and the expressions of degree-based topological indices are computed for these drugs by analyzing their molecular structure. The physicochemical properties of these are analyzed here through the QSPR models. The predictive ability of these indices is studied using correlation analysis; based on that, the best QSPR models have been generated using regression analysis. The Randić index correlates well with molecular weight, molar refractivity, and polarizability. The symmetric division index shows a high

https://doi.org/10.1021/acsomega.4c08572
ACS Omega 2025, 10, 3640−3651

correlation value with the enthalpy of vaporization, and the harmonic index shows the best correlation with molar volume also. Based on these correlation data, QSPR models have been generated for the different physicochemical properties, and we have predicted the physicochemical properties of the newly approved drug givinostat by using these developed QSPR models. Using these models can help scientists identify the optimum compound with desired properties. These models can analyze a large number of compounds to identify the compound with desired properties, which can save time and money in the drug development process.

■ ASSOCIATED CONTENT

Data Availability Statement

All data analyzed during this study are included in this published article.

■ AUTHOR INFORMATION

Corresponding Author

Roy Santiago − *Department of Mathematics, School of Advanced Sciences, Vellore Institute of Technology, Vellore 632014, India;* orcid.org/0000-0002-5542-6581; Email: roy.santiago@vit.ac.in

Author

Jyothish K − *Department of Mathematics, School of Advanced Sciences, Vellore Institute of Technology, Vellore 632014, India;* orcid.org/0009-0005-8345-9996

Complete contact information is available at: https://pubs.acs.org/10.1021/acsomega.4c08572

Author Contributions

J.K.: conceptualization; writing original draft; validation; investigation; visualization; and methodology. R.S.: supervision; validation; and conceptualization.

Notes

The authors declare no competing financial interest.

■ ACKNOWLEDGMENTS

The authors are thankful to Vellore Institute of Technology for providing a facility to carry out research work. The financial support from Vellore Institute of Technology is highly acknowledged. Jyothish K also acknowledges the Department of Science and Technology (DST), India, for granting the Inspire Fellowship, DST/Inspire fellowship/2023/IF230142.

■ REFERENCES

(1) Emery, A. E. The muscular dystrophies. *Lancet* **2002**, *359* (9307), 687−695.
(2) Mercuri, E.; Bönnemann, C. G.; Muntoni, F. Muscular dystrophies. *Lancet* **2019**, *394* (10213), 2025−2038.
(3) Rahimov, F.; Kunkel, L. M. Cellular and molecular mechanisms underlying muscular dystrophy. *J. Cell Biol.* **2013**, *201* (4), 499−510.
(4) Goyenvalle, A.; Seto, J. T.; Davies, K. E.; Chamberlain, J. Therapeutic approaches to muscular dystrophy. *Hum. Mol. Genet.* **2011**, *20* (R1), 69−78.
(5) Khurana, T. S.; Davies, K. E. Pharmacological strategies for muscular dystrophy. *Nat. Rev. Drug Discovery* **2003**, *2* (5), 379−390.
(6) McNally, E. M.; Pytel, P. Muscle diseases: the muscular dystrophies. *Annu. Rev. Pathol.:Mech. Dis.* **2007**, *2* (1), 87−109.
(7) Cohn, R. D.; Campbell, K. P. Molecular basis of muscular dystrophies. *Muscle Nerve* **2000**, *23* (10), 1456−1471.
(8) Leung, D. G.; Wagner, K. R. Therapeutic advances in muscular dystrophy. *Ann. Neurol.* **2013**, *74* (3), 404−411.
(9) Mercuri, E.; Muntoni, F. Muscular dystrophies. *Lancet* **2013**, *381* (9869), 845−860.
(10) Bez Batti Angulski, A.; Hosny, N.; Cohen, H.; Martin, A. A.; Hahn, D.; Bauer, J.; Metzger, J. M. Duchenne muscular dystrophy: Disease mechanism and therapeutic strategies. *Front. Physiol.* **2023**, *14*, 1183101.
(11) Emery, A. E. H. The muscular dystrophies. *Bmj* **1998**, *317* (7164), 991−995.
(12) Duan, D.; Goemans, N.; Takeda, S. I.; Mercuri, E.; Aartsma-Rus, A. Duchenne muscular dystrophy. *Nat. Rev. Dis. Prim.* **2021**, *7* (1), 13.
(13) Guiraud, S.; Davies, K. E. Pharmacological advances for treatment in Duchenne muscular dystrophy. *Curr. Opin. Pharmacol.* **2017**, *34*, 36−48.
(14) Aoki, Y.; Miyatake, S.; Shimizu-Motohashi, Y.; Takeda, S. Anti-inflammatory drugs for Duchenne muscular dystrophy: focus on skeletal muscle-releasing factors. *Drug Des. Dev. Ther.* **2016**, *10*, 2745−2758.
(15) Bello, L.; Pegoraro, E. The "usual suspects": genes for inflammation, fibrosis, regeneration, and muscle strength modify Duchenne muscular dystrophy. *J. Clin. Med.* **2019**, *8* (5), 649.
(16) Deconinck, N.; Dan, B. Pathophysiology of duchenne muscular dystrophy: current hypotheses. *Pediatr. Neurol.* **2007**, *36* (1), 1−7.
(17) Wilton-Clark, H.; Yokota, T. Recent trends in antisense therapies for Duchenne muscular dystrophy. *Pharmaceutics* **2023**, *15* (3), 778.
(18) Bushby, K.; et al. Diagnosis and management of Duchenne muscular dystrophy, part 1: diagnosis, and pharmacological and psychosocial management. *Lancet Neurol.* **2010**, *9* (1), 77−93.
(19) Reinig, A. M.; Mirzaei, S.; Berlau, D. J. Advances in the treatment of Duchenne muscular dystrophy: new and emerging pharmacotherapies. *Pharmacotherapy* **2017**, *37* (4), 492−499.
(20) Deng, J.; Zhang, J.; Shi, K.; Liu, Z. Drug development progress in duchenne muscular dystrophy. *Front. Pharmacol* **2022**, *13*, 950651.
(21) Malik, V.; Rodino-Klapac, L. R.; Mendell, J. R. Emerging drugs for Duchenne muscular dystrophy. *Expet Opin. Emerg. Drugs* **2012**, *17* (2), 261−277.
(22) Trinajstic, N. *Chemical Graph Theory*; CRC Press, 2018.
(23) Gutman, I. Degree-based topological indices. *Croat. Chem. Acta* **2013**, *86* (4), 351−361.
(24) Estrada, E.; Uriarte, E. Recent advances on the role of topological indices in drug discovery research. *Curr. Med. Chem.* **2001**, *8* (13), 1573−1588.
(25) Bokhary, S. A. U. H.; Adnan; Siddiqui, M. K.; Cancan, M. On topological indices and QSPR analysis of drugs used for the treatment of breast cancer. *Polycyclic Aromat. Compd.* **2022**, *42* (9), 6233−6253.
(26) Mahboob, A.; Rasheed, M. W.; Dhiaa, A. M.; Hanif, I.; Amin, L. On quantitative structure-property relationship (QSPR) analysis of physicochemical properties and anti-hepatitis prescription drugs using a linear regression model. *Heliyon* **2024**, *10* (4), No. e25908.
(27) Zhang, X.; Saif, M. J.; Idrees, N.; Kanwal, S.; Parveen, S.; Saeed, F. QSPR analysis of drugs for treatment of schizophrenia using topological indices. *ACS Omega* **2023**, *8* (44), 41417−41426.
(28) Jyothish, K.; Santiago, R.; Govardhan, S.; Hayat, S. Structure-property modeling of physicochemical properties of fractal trigonal triphenylenoids by means of novel degree-based topological indices. *Eur. Phys. J. E* **2024**, *47* (6), 42.
(29) Gonzalez-Diaz, H.; Vilar, S.; Santana, L.; Uriarte, E. Medicinal chemistry and bioinformatics-current trends in drugs discovery with networks topological indices. *Curr. Top. Med. Chem.* **2007**, *7* (10), 1015−1029.
(30) Ravi, V.; Desikan, K. Curvilinear regression analysis of benzenoid hydrocarbons and computation of some reduced reverse degree based topological indices for hyaluronic acid-paclitaxel conjugates. *Sci. Rep.* **2023**, *13* (1), 3239.
(31) Zaman, S.; Jalani, M.; Ullah, A.; Ahmad, W.; Saeedi, G. Mathematical analysis and molecular descriptors of two novel metal−organic models with chemical applications. *Sci. Rep.* **2023**, *13* (1), 5314.

(32) Hemmateenejad, B.; Yousefinejad, S.; Mehdipour, A. R. Novel amino acids indices based on quantum topological molecular similarity and their application to QSAR study of peptides. *Amino Acids* **2011**, *40*, 1169−1183.
(33) Havare, Ö. Ç. Topological indices and QSPR modeling of some novel drugs used in the cancer treatment. *Int. J. Quantum Chem.* **2021**, *121* (24), 26813.
(34) Gao, W.; Wang, W.; Farahani, M. R. Topological indices study of molecular structure in anticancer drugs. *J. Chem.* **2016**, *2016*, 1−8.
(35) Randic, M. Quantitative structure-property relationship Boiling points of planar benzenoids. *New J. Chem.* **1996**, *20* (10), 1001−1009.
(36) Mc, S.; Ns, B.; Kn, A. Predicting physico-chemical properties of octane isomers using QSPR approach. *Malaya J. Matematik* **2020**, *8* (1), 104−116.
(37) Varmuza, K.; Dehmer, M.; Bonchev, D. *Statistical Modelling of Molecular Descriptors in QSAR/QSPR*; Wiley Online Library, 2012.
(38) Jeyaraj, S. V.; Santiago, R. A study on efficient technique for generating vertex-based topological characterization of boric acid 2D structure. *ACS Omega* **2023**, *8* (25), 23089−23097.
(39) Yang, H.; Hanif, M. F.; Siddiqui, M. K.; Hanif, M. F.; Maqbool, A.; Fiidow, M. A. On analysis of topological indices and heat of formation for benzyl sulfamoyl network via curve fitting model. *Sci. Rep.* **2024**, *14* (1), 15526.
(40) Yousefinejad, S.; Hemmateenejad, B. Chemometrics tools in QSAR/QSPR studies: A historical perspective. *Chemom. Intell. Lab. Syst.* **2015**, *149*, 177−204.
(41) Kearnes, S.; McCloskey, K.; Berndl, M.; Pande, V.; Riley, P. Molecular graph convolutions: moving beyond fingerprints. *J. Comput. Aided Mol. Des.* **2016**, *30*, 595−608.
(42) Gutman, I.; Trinajstić, N. Graph theory and molecular orbitals.Total ϕ-electron energy of alternant hydrocarbons. *Chem. Phys. Lett.* **1972**, *17* (4), 535−538.
(43) Gutman, I.; Trinajstić, N.; Wilcox, C. F. Graph theory and molecular orbitals. XII. Acyclic polyenes. *J. Chem. Phys.* **1975**, *62* (9), 3399−3405.
(44) Randic, M. Characterization of molecular branching. *J. Am. Chem. Soc.* **1975**, *97* (23), 6609−6615.
(45) Gutman, I.; Furtula, B.; Elphick, C. Three new/old vertex-degree-based topological indices. In *MATCH Communications in Mathematical and in Computer Chemistry*; Faculty of Science & University of Kragujevac, 2014.
(46) Ali, A.; Gutman, I.; Furtula, B.; Redžepović, I.; Došlić, T.; Raza, Z. Augmented Zagreb index: extremal results and bounds. *Match Communications Math. Comput. Chem.* **2024**, *92*, 271−314.
(47) Shirdel, G. H.; Rezapour, H.; Sayadi, A. M. The hyper-Zagreb index of graph operations. *Iran. J. Math. Chem.* **2013**, *4* (2), 213−220.
(48) Fajtlowicz, S. On conjectures of Graffiti-II. *Congr. Numer.* **1987**, *60* (3), 187−197.
(49) Zhong, L. The harmonic index for graphs. *Appl. Math. Lett.* **2012**, *25* (3), 561−566.
(50) Vukičević, D.; Furtula, B. Topological index based on the ratios of geometrical and arithmetical means of end-vertex degrees of edges. *J. Math. Chem.* **2009**, *46*, 1369−1376.
(51) Zhou, B.; Trinajstić, N. On a novel connectivity index. *J. Math. Chem.* **2009**, *46* (4), 1252−1270.
(52) Du, Z.; Zhou, B.; Trinajstić, N. On the general sum-connectivity index of trees. *Appl. Math. Lett.* **2011**, *24* (3), 402−405.
(53) Vukicevic, D.; Gasperov, M. Bond additive modeling 1. Adriatic indices. *Croat. Chem. Acta* **2010**, *83* (3), 243−260.
(54) Sedlar, J.; Stevanović, D.; Vasilyev, A. On the inverse sum indeg index. *Discrete Appl. Math.* **2015**, *184*, 202−212.
(55) Estrada, E.; Torres, L.; Rodriguez, L.; Gutman, I. *An Atom-Bond Connectivity Index: Modelling the Enthalpy of Formation of Alkanes*; NISCAIR-CSIR, 1998.
(56) Drachman, D. B.; Toyka, K. V.; Myer, E. Prednisone in Duchenne muscular dystrophy. *Lancet* **1974**, *304* (7894), 1409−1412.
(57) Biggar, W. D.; Gingras, M.; Fehlings, D. L.; Harris, V. A.; Steele, C. A. Deflazacort treatment of Duchenne muscular dystrophy. *J. Pediatr.* **2001**, *138* (1), 45−50.
(58) Fenichel, G. M.; et al. Long-term benefit from prednisone therapy in Duchenne muscular dystrophy. *Neurology* **1991**, *41* (12), 1874.
(59) Biggar, W. D.; Harris, V. A.; Eliasoph, L.; Alman, B. Long-term benefits of deflazacort treatment for boys with Duchenne muscular dystrophy in their second decade. *Neuromuscul. Disord.* **2006**, *16* (4), 249−255.
(60) McDonald, C. M.; et al. Ataluren in patients with nonsense mutation Duchenne muscular dystrophy (ACT DMD): a multicentre, randomised, double-blind, placebo-controlled, phase 3 trial. *Lancet* **2017**, *390* (10101), 1489−1498.
(61) Shirley, M. Casimersen: first approval. *Drugs* **2021**, *81*, 875−879.
(62) Porte-Thomé, F.; Nagaraju, K.; Yu, Q.; Tatem, K.; Bkaily, G.; Scholz, W.; Slade, A.; Bot, N.; Kant, C. Development of Rimeporide, a sodium-hydrogen exchanger (NHE-1) inhibitor, for patients with Duchenne muscular dystrophy. *Neuromuscul. Disord.* **2015**, *25*, 259−260.
(63) Ciccone, I. *FDA Approves Vamorolone as a Treatment for Duchenne Muscular Dystrophy*; Neurology Live, 2023.
(64) Keam, S. J. Vamorolone: first approval. *Drugs* **2024**, *84* (1), 111−117.
(65) Buyse, G. M.; et al. Idebenone as a novel, therapeutic approach for Duchenne muscular dystrophy: results from a 12 month, double-blind, randomized placebo-controlled trial. *Neuromuscul. Disord.* **2011**, *21* (6), 396−405.
(66) McDonald, C. M.; et al. Idebenone reduces respiratory complications in patients with Duchenne muscular dystrophy. *Neuromuscul. Disord.* **2016**, *26* (8), 473−480.
(67) Bettica, P.; et al. Histological effects of givinostat in boys with Duchenne muscular dystrophy. *Neuromuscul. Disord.* **2016**, *26* (10), 643−649.
(68) Mercuri, E.; et al. Safety and efficacy of givinostat in boys with Duchenne muscular dystrophy (EPIDYS): a multicentre, randomised, double-blind, placebo-controlled, phase 3 trial. *Lancet Neurol.* **2024**, *23* (4), 393−403.
(69) Draper, N. R.; Smith, H. *Applied Regression Analysis*; John Wiley & Sons, 1998; Vol. *326*.
(70) Montgomery, D. C.; Peck, E. A.; Vining, G. G. *Introduction to Linear Regression Analysis*; John Wiley & Sons., 2021.
(71) Seber, G. A.; Lee, A. J. *Linear Regression Analysis*; John Wiley & Sons., 2012.
(72) https://pubchem.ncbi.nlm.nih.gov/.
(73) http://www.chemspider.com/.

https://doi.org/10.1021/acsomega.4c08572
ACS Omega 2025, 10, 3640−3651